

Mapping out the Relative Influence of Hydrogen and Halogen Bonds in Crystal Structures of a Family of Amide-Substituted Pyridines

Amila M. Abeysekera, Victor W. Day, Abhijeet S. Sinha, and Christer B. Aakeröy*

Cite This: <https://dx.doi.org/10.1021/acs.cgd.0c01086>

Read Online

ACCESS |



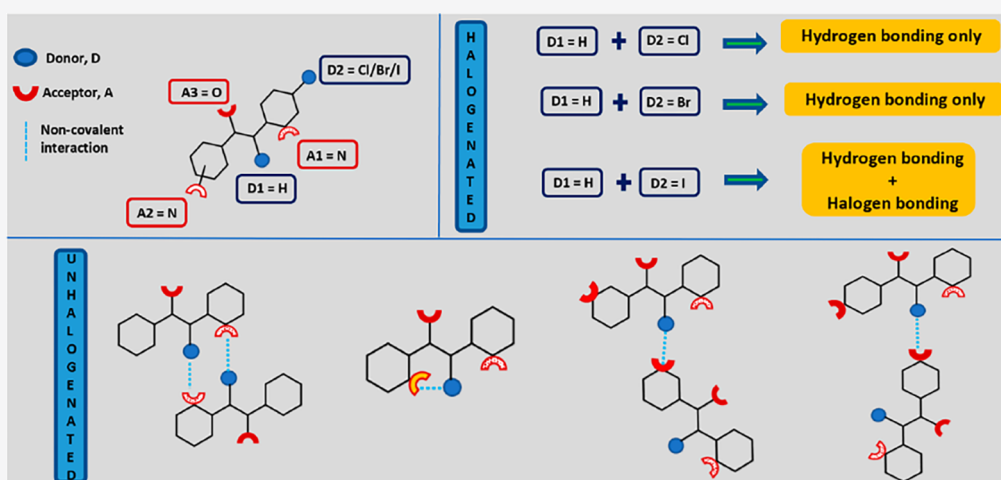
Metrics & More



Article Recommendations



Supporting Information



ABSTRACT: The simultaneous use of hydrogen bonds and halogen bonds in crystal engineering strategies has previously been employed in order to generate new solid forms with applications in e.g. pharmaceutical and agrochemical industries. Unfortunately, it is not easy to predict how these will coexist or compete in systems where multiple structural outcomes are possible. To address this challenge, we have investigated the solid-state landscape of a family of amide-substituted pyridines, belonging to four series, *N*-(pyridin-2-yl)benzamides (**Bz**), *N*-(pyridin-2-yl)picolinamides (**2Pyr**), *N*-(pyridin-2-yl)nicotinamides (**3Pyr**) and *N*-(pyridin-2-yl)isonicotinamides (**4Pyr**), functionalized with three different halogen atoms (chlorine, bromine, and iodine). We analyzed crystal structures of 16 compounds and identified their primary intermolecular interactions. Within each series, the chlorinated and brominated compounds present the same primary hydrogen-bond interactions as shown by the nonhalogenated parent. The *N*-(pyridin-2-yl)benzamides assembled via $\text{NH}\cdots\text{N}(\text{Py})$ synthons to form dimers, *N*-(pyridin-2-yl)picolinamides showed intramolecular $\text{N}-\text{H}\cdots\text{N}(\text{Py})$ hydrogen bonding, and both *N*-(pyridin-2-yl)nicotinamides (**3Pyr**) and *N*-(pyridin-2-yl)isonicotinamides (**4Pyr**) assembled via $\text{NH}\cdots\text{N}(\text{Py})$ synthons leading to the formation of chains or four-membered rings. In three out of the four series (**Bz**, **2Pyr**, and **4Pyr**) the chloro and bromo compounds were isostructural. Three out of the four iodinated compounds exhibited halogen bonds to a neighboring molecule. In two of these compounds, **Bz-I** and **2Pyr-I**, the primary hydrogen bonding resembled that of the other members of the family, indicating that the interactions mediated via the iodine atom were complementary rather than competitive with the hydrogen bonds. Two polymorphs of **4Pyr-I** were found, and in both forms, a halogen bond was formed with the $\text{N}(\text{py})$ acceptor which was engaged in $\text{N}-\text{H}\cdots\text{N}$ hydrogen bonds in the other members of this family. Since iodine acted as a halogen-bond donor in four-fifths of the crystal structures of iodinated compounds, these results show that the solid-state assembly of analogue compounds capable of hydrogen bonding have a high likelihood of being altered even in the presence of a nonactivated iodine atom.

The hydrogen bond^{1,2} has long been established as the primary driver for intermolecular assembly and organization, but halogen^{3,4} and chalcogen bonds^{5,6} are now also being recognized as valuable tools in practical crystal engineering.⁷ All three interactions share a considerable reliance on electrostatics for both strength and directionality, but as most

Received: August 3, 2020

Revised: September 29, 2020

molecules contain multiple sites capable of forming electrostatically based intermolecular bonds, it is difficult to predict, *a priori*, what the most likely pairing/binding between electron-poor (donor) and electron-rich (acceptor) sites will be. As a result, even relatively simple and rigid molecules can produce drastically different molecular aggregates in the solid state (Figure 1), which creates considerable challenges for bottom-up supramolecular synthesis.^{8,9}

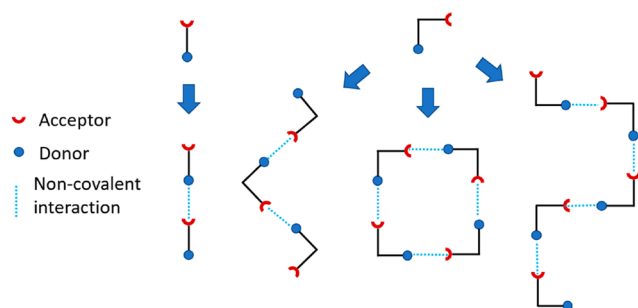


Figure 1. A few examples of intermolecular assembly based on the relative orientations of donor and acceptor sites.

The relative orientation of molecules within a crystalline material ultimately plays an important role in the resulting physical properties and has significant implications for the performance of high-value solids such as pharmaceuticals.^{10–12} In addition, an improved understanding of interactions prevailing between individual components can also help to develop effective synthetic strategies for cocrystallizations.^{13,14} A key concept that has become very helpful for identifying frequently occurring molecular recognition events in the solid state is the “synthon”: “a structural unit within a supermolecule which can be formed and/or assembled by known or conceivable synthetic operations involving intermolecular interactions”.¹⁵ In order to further transition this concept into versatile and reliable synthetic strategies, we need systematic structural studies on closely related compounds so that we directly connect functional groups and molecular structure to specific and predictable molecular recognition events in the solid state.^{16–19}

It has been shown that the preferred synthon in a competitive assembly can often be rationalized using calculated molecular electrostatic potentials (MEPs), where the best acceptor (presenting the largest negative MEP) interacts with the best donor (presenting the most positive MEP) on the molecular

surface).²⁰ However, in systems with donors of different elements (e.g. hydrogen and halogen), and where acceptors are not of the same element, a direct comparison of electrostatic potentials alone may not lead to reliable protocols for identifying which synthons are most likely to appear in the resulting crystal structure. Detailed studies that address such questions are relatively rare, and therefore we have carried out a systematic structural examination of four complementary series of relatively simple organic molecules that contain a variety of hydrogen-bond/halogen-bond donors and acceptors in order to map out the structural landscape of the amide group. Related studies include work on methyl-*N*-(pyridyl)benzamides,²¹ fluoro-*N*-(pyridyl)benzamides,²² and monochlorobenzamides,²³ where $N-H\cdots N$ interactions were shown to dominate over $N-H\cdots O=C$ interactions. However, the molecules under consideration in those studies include only one pyridine nitrogen and do not include iodine, which is the halogen atom most capable of eliciting halogen bonding.²⁴

In this study, 16 molecules grouped into four series (**Bz**, **2Pyr**, **3Pyr**, and **4Pyr**) have been structurally interrogated by increasing the supramolecular and steric complexity (Figure 2).

In the course of this work we wanted to address several key questions regarding molecular aggregation and recognition, including to what extent MEPs can help to rationalize observed synthons and whether the presence of a halogen atom can significantly alter the supramolecular assembly and, if so, will all halogen atoms have the same effect (Figure 2). To the best of our knowledge, there have been no systematic structural studies of hydrogen-bond motifs in the solid state of molecules bearing the core structure (i.e. the unhalogenated compound) of the **Bz** series. Reported structures²⁵ to date bearing the **2Pyr** core structure mainly form assemblies within larger molecules²⁶ and contain only fluorine as a halogen atom substituent.²⁷ The **3Pyr** and **4Pyr** core structures (unhalogenated compounds) have been utilized in metal complexation,²⁸ but exhaustive data on the solid-state self-assembly of these compounds with potential halogen-bond donors have not been reported.

In addition, we wanted to establish which of the two most likely motifs, chains or dimers (Figure 3), will prevail in the **Bz** series and how the assembly process is affected by increasing molecular complexity and steric variability by the addition of a competing acceptor site as in the series **2Pyr**, **3Pyr**, and **4Pyr**, respectively. The most likely interactions and the resulting aggregates are presented schematically in Figure 3.

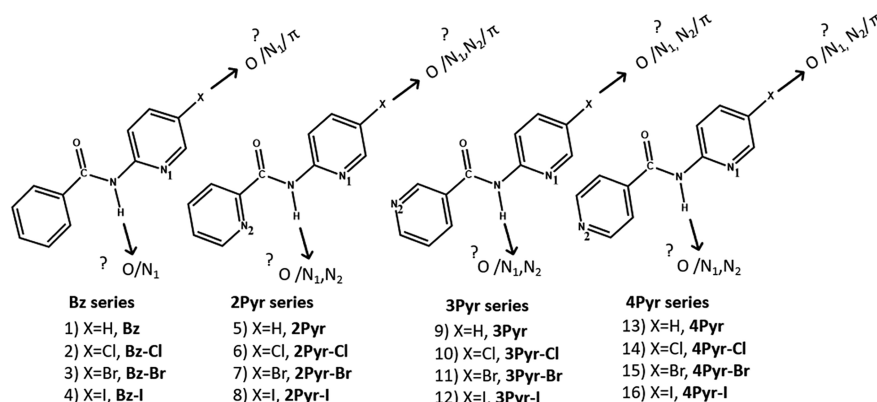


Figure 2. Molecular structures of compounds in this study and likely sites of binding for amide hydrogen and the halogen atom in each case.

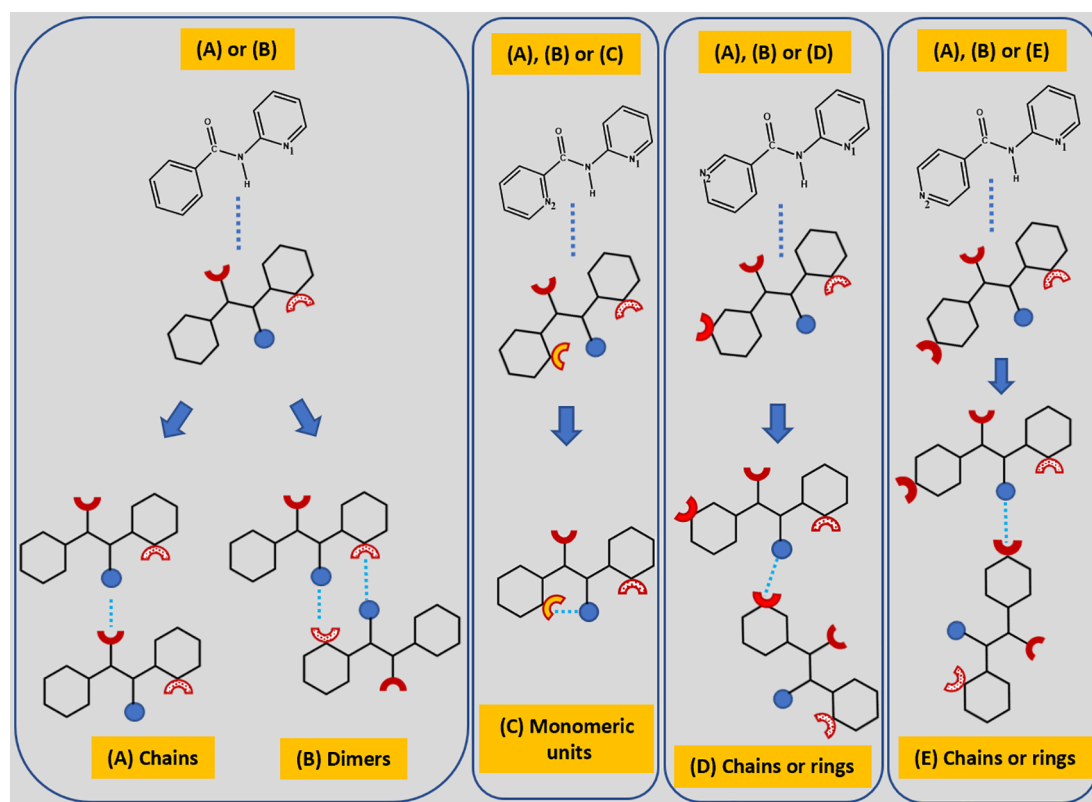


Figure 3. Schematic representation of possible structural consequences of increasing the number of acceptor sites and their relative positions.

EXPERIMENTAL SECTION

Bz Series. The synthesis of *N*-(pyridin-2-yl)benzamides was done according to an available literature procedure.²⁹

Synthesis of *N*-(Pyridin-2-yl)benzamide. 2-Aminopyridine (1.03 g, 11.0 mmol) was dissolved in 50 mL of pyridine and cooled in an ice bath. Benzoyl chloride (1.85 mL, 16.0 mmol) was added dropwise, and the temperature was maintained between 0 and 5 °C. After the addition was complete, the solution was stirred at room temperature until no further starting material (2-amino-5-pyridine) was detected by TLC. Upon completion, chilled water (100 mL) was added and the mixture stirred for 15 min. The reaction contents were extracted with dichloromethane. The organic layer was washed with saturated sodium bicarbonate solution, brine, and water, dried with anhydrous magnesium sulfate, filtered, and concentrated in vacuo to isolate the pure product. Yield: 80%. Mp: 92–94 °C. (lit. mp 80–82 °C).³⁰ ¹H NMR (400 MHz, DMSO-*d*₆): δ 10.78 (s, 1H), 8.44–8.35 (m, 1H), 8.20 (dd, *J* = 8.4, 1.1 Hz, 1H), 8.07–8.00 (m, 2H), 7.88–7.79 (m, 1H), 7.59 (td, *J* = 7.3, 1.3 Hz, 1H), 7.51 (ddd, *J* = 8.4, 6.7, 1.3 Hz, 2H), 7.16 (ddd, *J* = 7.4, 4.8, 1.1 Hz, 1H). ¹³C NMR (101 MHz, DMSO-*d*₆): δ 166.46, 152.68, 148.40, 138.57, 134.57, 132.38, 128.81(2C), 128.46(2C), 120.26, 115.20

Synthesis of *N*-(5-Chloropyridin-2-yl)benzamide. 2-Amino-5-chloropyridine (1.40 g, 11.0 mmol) was dissolved in 50 mL of pyridine and cooled in an ice bath. Benzoyl chloride (1.85 mL, 16.0 mmol) was added dropwise, and the temperature was maintained between 0 and 5 °C. After the addition was complete, the contents were stirred at room temperature until no further starting material (2-amino-5-chloropyridine) was detected by TLC. Upon completion, chilled water (100 mL) was added and the mixture stirred for 15 min. The reaction contents were extracted with dichloromethane, and the organic layer was washed with saturated sodium bicarbonate solution, brine, and water, dried with anhydrous magnesium sulfate, filtered, and concentrated in vacuo to isolate the pure product. Yield: 85%. Mp: 123–125 °C (lit. mp 124–125 °C).³¹ ¹H NMR (400 MHz, DMSO-*d*₆): δ 10.99 (s, 1H), 8.44 (d, *J* = 2.7 Hz, 1H), 8.25 (d, *J* = 8.9 Hz, 1H), 8.03 (dt, *J* = 7.1, 1.4 Hz, 2H), 7.95 (dd, *J* = 9.0, 2.7 Hz, 1H), 7.64–7.55 (m, 1H), 7.51 (dd, *J* = 8.2, 6.8

Hz, 2H). ¹³C NMR (101 MHz, DMSO-*d*₆): δ 166.56, 151.36, 146.73, 138.28, 134.28, 132.52, 128.81, 128.52, 126.00, 116.24.

Synthesis of *N*-(5-Bromopyridin-2-yl)benzamide. 2-Amino-5-bromopyridine (1.90 g, 11.0 mmol) was dissolved in 50 mL of pyridine and cooled in an ice bath. Benzoyl chloride (1.85 mL, 16.0 mmol) was added dropwise, and the temperature was maintained between 0 and 5 °C. After the addition was complete, the contents were stirred at room temperature until no further starting material (2-amino-5-bromopyridine) was detected by TLC. Upon completion, chilled water (100 mL) was added and the mixture stirred for 15 min. The reaction contents were extracted with dichloromethane, and the organic layer was washed with saturated sodium bicarbonate solution, brine, and water, dried with anhydrous magnesium sulfate, filtered, and concentrated in vacuo to isolate the pure product. Yield: 82%. Mp: 119–121 °C (lit. mp 223 °C).^{29,32} ¹H NMR (400 MHz, DMSO-*d*₆): δ 10.98 (s, 1H), 8.55–8.48 (m, 1H), 8.19 (dd, *J* = 8.9, 0.7 Hz, 1H), 8.07 (dd, *J* = 8.9, 2.6 Hz, 1H), 8.06–7.98 (m, 2H), 7.64–7.56 (m, 1H), 7.55–7.47 (m, 2H). ¹³C NMR (101 MHz, DMSO-*d*₆): δ 166.17, 151.24, 148.52, 140.61, 133.86, 132.13, 128.42, 128.10, 116.36, 114.02.

Synthesis of *N*-(5-Iodopyridin-2-yl)benzamide. 2-Amino-5-iodopyridine (2.20 g, 11.0 mmol) was dissolved in 50 mL of pyridine and cooled in an ice bath. Benzoyl chloride (1.85 mL, 16.0 mmol) was added dropwise, and the temperature was maintained between 0 and 5 °C. After the addition was complete, the solution was stirred at room temperature until no further starting material (2-amino-5-iodopyridine) was detected by TLC. Upon completion, chilled water (100 mL) was added and the mixture stirred for 15 min. The reaction contents were extracted with dichloromethane, and the organic layer was washed with saturated sodium bicarbonate solution, brine, and water, dried with anhydrous magnesium sulfate, filtered, and concentrated in vacuo to isolate the pure product. Yield 85%, Mp: 121–123 °C (lit. mp 121–122 °C).³³ ¹H NMR (400 MHz, DMSO-*d*₆): δ 10.92 (s, 1H), 8.60 (d, *J* = 2.3 Hz, 1H), 8.17 (dd, *J* = 8.8, 2.3 Hz, 1H), 8.09 (d, *J* = 8.8 Hz, 1H), 8.02 (dd, *J* = 8.2, 1.4 Hz, 2H), 7.64–7.55 (m, 1H), 7.50 (t, *J* = 7.5 Hz, 2H). ¹³C NMR (101 MHz, DMSO-*d*₆): δ 166.55, 153.85, 151.90, 146.36, 134.31, 132.52, 128.81, 128.50, 117.16, 87.21.

2Pyr Series. The synthesis of *N*-(pyridin-2-yl)picolinamides was done according to an available literature procedure.³⁴

Synthesis of *N*-(Pyridin-2-yl)picolinamide. Picolinic acid (1.00 g, 8.13 mmol), 2-(1*H*-benzotriazol-1-yl)-1,1,3,3-tetramethyluronium hexafluorophosphate (4.00 g, 10.5 mmol), triethylamine (3.40 mL, 24.4 mmol), and 2-aminopyridine (0.836 g, 8.90 mmol) were dissolved in 60 mL of DMF. The reactants were stirred at room temperature for 14 h, diluted with ethyl acetate, and washed with water. The organic layer was dried with anhydrous magnesium sulfate and concentrated by rotary evaporation to obtain the crude product, which was purified by column chromatography using hexane/ethyl acetate (90/10) as eluent to obtain the pure product. Yield 50%. Mp: 117–119 °C (lit. mp 107–108 °C).³⁵ ¹H NMR (400 MHz, DMSO-*d*₆): δ 10.43 (s, 1H), 8.77 (ddd, *J* = 4.8, 1.7, 1.0 Hz, 1H), 8.44–8.37 (m, 1H), 8.29 (dt, *J* = 8.3, 1.0 Hz, 1H), 8.22 (dt, *J* = 7.8, 1.1 Hz, 1H), 8.12 (td, *J* = 7.7, 1.7 Hz, 1H), 7.91 (ddd, *J* = 8.8, 7.3, 1.9 Hz, 1H), 7.74 (ddd, *J* = 7.6, 4.7, 1.3 Hz, 1H), 7.22 (ddd, *J* = 7.4, 4.9, 1.0 Hz, 1H). ¹³C NMR (101 MHz, DMSO-*d*₆): δ 161.55, 150.15, 148.35, 148.08, 138.28, 138.14, 127.20, 121.86, 119.88, 112.74.

Synthesis of *N*-(5-Chloropyridin-2-yl)picolinamide. Picolinic acid (1.00 g, 8.13 mmol), 2-(1*H*-benzotriazol-1-yl)-1,1,3,3-tetramethyluronium hexafluorophosphate (4.00 g, 10.5 mmol), triethylamine (3.40 mL, 24.4 mmol), and 2-amino-5-chloropyridine (1.14 g, 8.90 mmol) were dissolved in 60 mL of DMF. The reactants were stirred at room temperature for 14 h, diluted with ethyl acetate, and washed with water. The organic layer was dried with anhydrous magnesium sulfate and concentrated by rotary evaporation to obtain the crude product, which was purified by column chromatography using hexane/ethyl acetate (90/10) as eluent to obtain the pure product. Yield 55%. Mp: 153–155 °C. ¹H NMR (400 MHz, DMSO-*d*₆): δ 10.53 (s, 1H), 8.76 (ddd, *J* = 4.8, 1.7, 0.9 Hz, 1H), 8.46 (dd, *J* = 2.6, 0.7 Hz, 1H), 8.31 (dd, *J* = 8.9, 0.7 Hz, 1H), 8.22 (dt, *J* = 7.8, 1.1 Hz, 1H), 8.12 (td, *J* = 7.7, 1.7 Hz, 1H), 8.04 (dd, *J* = 8.9, 2.6 Hz, 1H), 7.74 (ddd, *J* = 7.6, 4.8, 1.3 Hz, 1H). ¹³C NMR (101 MHz, DMSO-*d*₆): δ 162.76, 149.93, 149.45, 148.94, 147.51, 139.23, 139.06, 128.38, 126.66, 123.05, 115.00.

Synthesis of *N*-(5-Bromopyridin-2-yl)picolinamide. Picolinic acid (1.00 g, 8.13 mmol), 2-(1*H*-benzotriazol-1-yl)-1,1,3,3-tetramethyluronium hexafluorophosphate (4.00 g, 10.5 mmol), triethylamine (3.40 mL, 24.4 mmol), and 2-amino-5-bromopyridine (1.54 g, 8.90 mmol) were dissolved in 60 mL of DMF. The reactants were stirred at room temperature for 14 h, diluted with ethyl acetate, and washed with water. The organic layer was dried with anhydrous magnesium sulfate and concentrated by rotary evaporation to obtain the crude product, which was purified by column chromatography using hexane/ethyl acetate (90/10) as eluent to obtain the pure product. Yield: 53%. Mp: 149–151 °C. ¹H NMR (400 MHz, DMSO-*d*₆): δ 10.50 (s, 1H), 8.74 (d, *J* = 4.8 Hz, 1H), 8.50 (d, *J* = 2.5 Hz, 1H), 8.22 (dd, *J* = 17.5, 8.3 Hz, 2H), 8.16–8.06 (m, 2H), 7.73 (dd, *J* = 7.6, 4.8 Hz, 1H) ¹³C NMR (101 MHz, DMSO-*d*₆): δ 162.76, 150.22, 149.68, 149.43, 148.93, 141.76, 139.21, 128.38, 123.04, 115.50, 115.05.

Synthesis of *N*-(5-Iodopyridin-2-yl)picolinamide. Picolinic acid (1.00 g, 8.13 mmol), 2-(1*H*-benzotriazol-1-yl)-1,1,3,3-tetramethyluronium hexafluorophosphate (4.00 g, 10.5 mmol), triethylamine (3.40 mL, 24.4 mmol), and 2-amino-5-iodopyridine (1.96 g, 8.90 mmol) were dissolved in 60 mL of DMF. The reactants were stirred at room temperature for 14 h, diluted with ethyl acetate, and washed with water. The organic layer was dried with anhydrous magnesium sulfate and concentrated by rotary evaporation to obtain the crude product, which was purified by column chromatography using hexane/ethyl acetate (90/10) as eluent to obtain the pure product. Yield: 55%. Mp: 124–126 °C. ¹H NMR (400 MHz, DMSO-*d*₆): δ 10.46 (s, 1H), 8.75 (ddd, *J* = 4.8, 1.7, 0.9 Hz, 1H), 8.60 (dd, *J* = 2.2, 0.8 Hz, 1H), 8.27–8.17 (m, 2H), 8.12 (ddd, *J* = 15.6, 8.1, 1.3 Hz, 2H), 7.73 (ddd, *J* = 7.5, 4.8, 1.3 Hz, 1H). ¹³C NMR (101 MHz, DMSO-*d*₆): δ 162.56, 154.39, 150.23, 149.22, 148.76, 146.90, 139.00, 128.15, 122.81, 115.67, 87.70.

3Pyr Series. The synthesis of *N*-(pyridin-2-yl)nicotinamides was done according to an available literature procedure.³⁶

Synthesis of *N*-(Pyridin-2-yl)nicotinamide. Nicotinic acid (1.21 g, 9.83 mmol) and triethylamine (1.40 mL, 10.0 mmol) were added to 30 mL of chloroform and cooled in an ice bath. Thionyl chloride (0.73 mL, 10.0 mmol) was added dropwise under nitrogen. After the addition

of thionyl chloride was complete, the mixture was heated under reflux for 3 h. The mixture was cooled to room temperature, and a solution of 2-aminopyridine (0.94 g, 10.0 mmol) and triethylamine (1.40 mL, 10.0 mmol) in 30 mL of acetonitrile was added in situ. The contents were stirred overnight at room temperature. The organic layer was washed with water and the solvent removed in vacuo. The product was purified by column chromatography using hexane/ethyl acetate (90/10) as eluent to isolate the pure product. Yield 28%. Mp: 137–139 °C (lit. mp 136–137 °C).³⁶ ¹H NMR (400 MHz, DMSO-*d*₆): δ 11.07 (s, 1H), 9.13 (dd, *J* = 2.4, 0.9 Hz, 1H), 8.75 (dd, *J* = 4.8, 1.7 Hz, 1H), 8.40 (ddd, *J* = 4.8, 2.0, 0.9 Hz, 1H), 8.37–8.30 (m, 1H), 8.19 (dt, *J* = 8.4, 1.0 Hz, 1H), 7.86 (ddd, *J* = 8.5, 7.4, 2.0 Hz, 1H), 7.54 (ddd, *J* = 8.0, 4.8, 0.9 Hz, 1H), 7.19 (ddd, *J* = 7.4, 4.8, 1.0 Hz, 1H). ¹³C NMR (101 MHz, DMSO-*d*₆): δ 165.40, 153.00, 152.61, 149.68, 148.68, 138.91, 136.41, 130.55, 124.07, 120.75, 115.40.

Synthesis of *N*-(5-Chloropyridin-2-yl)nicotinamide. Nicotinic acid (1.21 g, 9.83 mmol) and triethylamine (1.40 mL, 10.0 mmol) were added to 30 mL of chloroform and cooled in an ice bath. Thionyl chloride (0.73 mL, 10.0 mmol) was added dropwise under nitrogen. After the addition of thionyl chloride was complete, the mixture was heated under reflux for 3 h. The mixture was cooled to room temperature, and a solution of 2-amino-5-chloropyridine (1.28 g, 10.0 mmol) and triethylamine (1.40 mL, 10.0 mmol) in 30 mL of acetonitrile was added in situ. The contents were stirred overnight at room temperature. The organic layer was washed with water and the solvent removed in vacuo. The product was purified by column chromatography using hexane/ethyl acetate (90/10) as eluent to isolate the pure product. Yield: 28%. Mp: 193–195 °C. ¹H NMR (400 MHz, DMSO-*d*₆): δ 11.27 (s, 1H), 9.13 (d, *J* = 2.3 Hz, 1H), 8.76 (dd, *J* = 4.9, 1.7 Hz, 1H), 8.47 (d, *J* = 2.7 Hz, 1H), 8.34 (dt, *J* = 8.0, 2.0 Hz, 1H), 8.24 (d, *J* = 8.9 Hz, 1H), 7.99 (dd, *J* = 8.9, 2.7 Hz, 1H), 7.59–7.51 (m, 1H). ¹³C NMR (101 MHz, DMSO-*d*₆): δ 164.92, 152.51, 150.69, 149.09, 146.45, 138.03, 135.87, 129.73, 125.87, 123.47, 115.85.

Synthesis of *N*-(5-Bromopyridin-2-yl)nicotinamide. Nicotinic acid (1.21 g, 9.83 mmol) and triethylamine (1.40 mL, 10.0 mmol) were added to 30 mL of chloroform and cooled in an ice bath. Thionyl chloride (0.73 mL, 10.0 mmol) was added dropwise under nitrogen. After the addition of thionyl chloride was complete, the mixture was heated under reflux for 3 h. The mixture was cooled to room temperature, and a solution of 2-amino-5-bromopyridine (1.73 g, 10.0 mmol) and triethylamine (1.40 mL, 10.0 mmol) in 30 mL of acetonitrile was added in situ. The contents were stirred overnight at room temperature. The organic layer was washed with water and the solvent removed in vacuo. The product was purified by column chromatography using hexane/ethyl acetate (90/10) as eluent to isolate the pure product. Yield: 28%. Mp: 190–192 °C. ¹H NMR (400 MHz, DMSO-*d*₆): δ 11.25 (s, 1H), 9.12 (dd, *J* = 2.4, 0.9 Hz, 1H), 8.75 (dd, *J* = 4.8, 1.7 Hz, 1H), 8.57–8.50 (m, 1H), 8.37–8.29 (m, 1H), 8.19 (dd, *J* = 8.9, 0.8 Hz, 1H), 8.09 (dd, *J* = 8.9, 2.5 Hz, 1H), 7.54 (ddd, *J* = 8.0, 4.8, 0.9 Hz, 1H), 2.08 (s, 2H). ¹³C NMR (101 MHz, DMSO-*d*₆): δ 164.92, 152.51, 150.99, 149.09, 148.62, 140.75, 135.85, 129.72, 123.45, 116.34, 114.30, 30.73.

Synthesis of *N*-(5-Iodopyridin-2-yl)nicotinamide. Nicotinic acid (1.21 g, 9.83 mmol) and triethylamine (1.40 mL, 10.0 mmol) were added to 30 mL of chloroform and cooled in an ice bath. Thionyl chloride (0.73 mL, 10.0 mmol) was added dropwise under nitrogen. After the addition of thionyl chloride was complete, the mixture was heated under reflux for 3 h. The mixture was cooled to room temperature, and a solution of 2-amino-5-iodopyridine (2.20 g, 10.0 mmol) and triethylamine (1.40 mL, 10.0 mmol) in 30 mL of acetonitrile was added in situ. The contents were stirred overnight at room temperature. The organic layer was washed with water and the solvent removed in vacuo. The product was purified by column chromatography using hexane/ethyl acetate (90/10) as eluent to isolate the pure product. Yield: 25%. Mp: 192–194 °C. ¹H NMR (400 MHz, DMSO-*d*₆): δ 11.21 (s, 1H), 9.15–9.10 (m, 1H), 8.76 (dd, *J* = 4.8, 1.7 Hz, 1H), 8.65–8.60 (m, 1H), 8.34 (dt, *J* = 8.1, 2.0 Hz, 1H), 8.20 (dd, *J* = 8.8, 2.3 Hz, 1H), 8.12–8.05 (m, 1H), 7.55 (ddd, *J* = 8.0, 4.8, 0.9 Hz, 1H). ¹³C NMR (101 MHz, DMSO-*d*₆): δ 164.90, 153.53, 152.49, 151.24, 149.08, 146.09, 135.83, 129.75, 123.44, 116.72, 87.18.

4Pyr Series. The synthesis of *N*-(pyridin-2-yl)isonicotinamides was done according to an available literature procedure.³⁶

Synthesis of *N*-(Pyridin-2-yl)isonicotinamide. Isonicotinic acid (1.21 g, 9.83 mmol) and triethylamine (1.40 mL, 10.0 mmol) were added to 30 mL of chloroform and cooled in an ice bath. Thionyl chloride (0.73 mL, 10.0 mmol) was added dropwise under nitrogen. After the addition of thionyl chloride was complete, the mixture was heated under reflux for 3 h. The mixture was cooled to room temperature, and a solution of 2-aminopyridine (0.94 g, 10.0 mmol) and triethylamine (1.40 mL, 10.0 mmol) in 30 mL of acetonitrile was added in situ. The contents were stirred overnight at room temperature. The organic layer was washed with water and the solvent removed in vacuo. The product was purified by column chromatography using hexane/ethyl acetate (90/10) as eluent to isolate the pure product. Yield: 32%, Mp: 136–138 °C (lit. mp 136–138 °C).³⁶ ¹H NMR (400 MHz, DMSO-*d*₆): δ 8.77 (d, *J* = 6.0 Hz, 2H), 8.42 (d, *J* = 3.7 Hz, 1H), 8.19 (d, *J* = 8.3 Hz, 1H), 7.92 (d, *J* = 6.1 Hz, 2H), 7.88 (s, 1H), 7.22 (s, 1H). ¹³C NMR (101 MHz, DMSO-*d*₆): δ 164.94, 152.01, 150.49, 148.35, 141.50, 138.60, 122.08, 120.59, 115.15.

Synthesis of *N*-(5-Chloropyridin-2-yl)isonicotinamide. Isonicotinic acid (1.21 g, 9.83 mmol) and triethylamine (1.40 mL, 10.0 mmol) were added to 30 mL of chloroform and cooled in an ice bath. Thionyl chloride (0.73 mL, 10.0 mmol) was added dropwise under nitrogen. After the addition of thionyl chloride was complete, the mixture was heated under reflux for 3 h. The mixture was cooled to room temperature, and a solution of 2-amino-5-chloropyridine (1.28 g, 10.0 mmol) and triethylamine (1.40 mL, 10.0 mmol) in 30 mL of acetonitrile was added in situ. The contents were stirred overnight at room temperature. The organic layer was washed with water and the solvent removed in vacuo. The product was purified by column chromatography using hexane/ethyl acetate (90/10) as eluent to isolate the pure product. Yield: 30%. Mp: 158–160 °C. ¹H NMR (400 MHz, DMSO-*d*₆): δ 11.31 (s, 1H), 8.77 (d, *J* = 5.8 Hz, 2H), 8.47 (d, *J* = 2.6 Hz, 1H), 8.23 (d, *J* = 8.9 Hz, 1H), 7.99 (dd, *J* = 8.9, 2.7 Hz, 1H), 7.90 (d, *J* = 5.9 Hz, 2H). ¹³C NMR (101 MHz, DMSO-*d*₆): δ 165.01, 150.64, 150.44, 146.67, 141.18, 138.25, 126.28, 122.04, 116.15.

Synthesis of *N*-(5-Bromopyridin-2-yl)isonicotinamide. Isonicotinic acid (1.21 g, 9.83 mmol) and triethylamine (1.40 mL, 10.0 mmol) were added to 30 mL of chloroform and cooled in an ice bath. Thionyl chloride (0.73 mL, 10.0 mmol) was added dropwise under nitrogen. After the addition of thionyl chloride was complete, the mixture was heated under reflux for 3 h. The mixture was cooled to room temperature and a solution of 2-amino-5-bromopyridine (1.73 g, 10.0 mmol) and triethylamine (1.40 mL, 10.0 mmol) in 30 mL of acetonitrile was added in situ. The contents were stirred overnight at room temperature. The organic layer was washed with water and the solvent removed in vacuo. The product was purified by column chromatography using hexane/ethyl acetate (90/10) as eluent to isolate the pure product. Yield: 28%. Mp: 166–168 °C. ¹H NMR (400 MHz, DMSO-*d*₆): δ 11.30 (s, 2H), 8.80–8.74 (m, 4H), 8.54 (d, *J* = 2.5 Hz, 2H), 8.18 (d, *J* = 8.9 Hz, 2H), 8.10 (dd, *J* = 8.9, 2.5 Hz, 2H), 7.93–7.87 (m, 4H), 2.53–2.47 (m, 1H). ¹³C NMR (101 MHz, DMSO-*d*₆): δ 165.26, 151.18, 150.67, 149.09, 141.41, 141.22, 122.26, 116.88, 114.99.

Synthesis of *N*-(5-Iodopyridin-2-yl)isonicotinamide. Isonicotinic acid (1.21 g, 9.83 mmol) and triethylamine (1.40 mL, 10.0 mmol) were added to 30 mL of chloroform and cooled in an ice bath. Thionyl chloride (0.73 mL, 10.0 mmol) was added dropwise under nitrogen. After the addition of thionyl chloride was complete, the mixture was heated under reflux for 3 h. The mixture was cooled to room temperature, and a solution of 2-amino-5-iodopyridine (2.20 g, 10.0 mmol) and triethylamine (1.40 mL, 10.0 mmol) in 30 mL of acetonitrile was added in situ. The contents were stirred overnight at room temperature. The organic layer was washed with water and the solvent removed in vacuo. The product was purified by column chromatography using hexane/ethyl acetate (90/10) as eluent to isolate the pure product. Yield: 30%. Mp: 194–196 °C. ¹H NMR (400 MHz, DMSO-*d*₆): δ 11.25 (s, 1H), 8.81–8.74 (m, 2H), 8.63 (dd, *J* = 2.4, 0.8 Hz, 1H), 8.21 (dd, *J* = 8.7, 2.3 Hz, 1H), 8.08 (dd, *J* = 8.8, 0.8 Hz, 1H), 7.93–7.87 (m, 2H). ¹³C NMR (101 MHz, DMSO-*d*₆): δ 165.04, 153.80, 151.24, 150.47, 146.38, 141.25, 122.05, 117.05, 87.72.

In order to obtain crystals suitable for single-crystal X-ray diffraction, slow evaporation from a variety of solvents was used for all 16 compounds (Table 1).

Table 1. Solvents Used for Crystal Growth and Crystal Descriptions^a

compound	code	solvent	color, morphology
<i>N</i> -(pyridin-2-yl)benzamide	Bz	ethanol	colorless, rectangular
<i>N</i> -(5-chloropyridin-2-yl)benzamide	Bz-Cl	ethanol	colorless, blocks
<i>N</i> -(5-bromopyridin-2-yl)benzamide	Bz-Br ³⁷	ethanol	colorless, blocks
<i>N</i> -(5-iodopyridin-2-yl)benzamide	Bz-I	ethanol	colorless, squares
<i>N</i> -(pyridin-2-yl)picolinamide	2Pyr	acetone	colorless, rectangular
<i>N</i> -(5-chloropyridin-2-yl)picolinamide	2Pyr-Cl	methanol/ethyl acetate (50/50)	colorless, rectangular
<i>N</i> -(5-bromopyridin-2-yl)picolinamide	2Pyr-Br	acetonitrile	colorless, needle
<i>N</i> -(5-iodopyridin-2-yl)picolinamide	2Pyr-I	hexane/ethyl acetate (80/20)	colorless, needle
<i>N</i> -(pyridin-2-yl)nicotinamide	3Pyr	toluene	colorless, rectangular
<i>N</i> -(5-chloropyridin-2-yl)nicotinamide	3Pyr-Cl	methanol	colorless needle
<i>N</i> -(5-bromopyridin-2-yl)nicotinamide	3Pyr-Br	methanol	yellow, rectangular
<i>N</i> -(5-iodopyridin-2-yl)nicotinamide	3Pyr-I	tetrahydrofuran	colorless, rectangular
<i>N</i> -(pyridin-2-yl)isonicotinamide	4Pyr ³⁸	methanol	yellow, plate
<i>N</i> -(5-chloropyridin-2-yl)isonicotinamide	4Pyr-Cl	toluene	colorless, rectangular
<i>N</i> -(5-bromopyridin-2-yl)isonicotinamide	4Pyr-Br	methanol	colorless, rectangular
<i>N</i> -(5-iodopyridin-2-yl)isonicotinamide	4Pyr-I-i	hexane/ethyl acetate (80/20)	yellow, parallelepiped
	4Pyr-I-ii ^b	ethyl acetate	colorless, needle

^aElectrostatic potentials were calculated with density functional theory at the B3LYP level using the 6-311++G** basis set under vacuum, using Spartan 08[†] software. Details of crystallographic experiments are given in the Supporting Information. ^bObtained from a failed cocrystallization experiment of 4Pyr-I with dodecanoic acid in 1:1 molar ratio.

RESULTS

The calculated MEP values are shown in Figure 4.

In every one of the four crystal structures from the Bz family, the primary intermolecular interaction is a N–H⋯N(py)/N(py)⋯H–N synthon that produced symmetry-related dimers (Figure 5a). The only additional interaction of note is a C–I⋯π halogen bond in Bz-I. The analogous chloro and bromo compounds do not display any other notable short contacts to neighboring molecules. The relevant hydrogen- and halogen-bond geometries in these four crystal structures are given in Table 2.

The primary noncovalent interactions in the four crystal structures from the 2Pyr series are shown in Figure 6. The addition of a pyridyl substituent with the nitrogen atom in close proximity to the N–H hydrogen-bond donor of the amide moiety leads to the formation of a very persistent N–H⋯N(py) intramolecular interaction in all four structures, which effectively

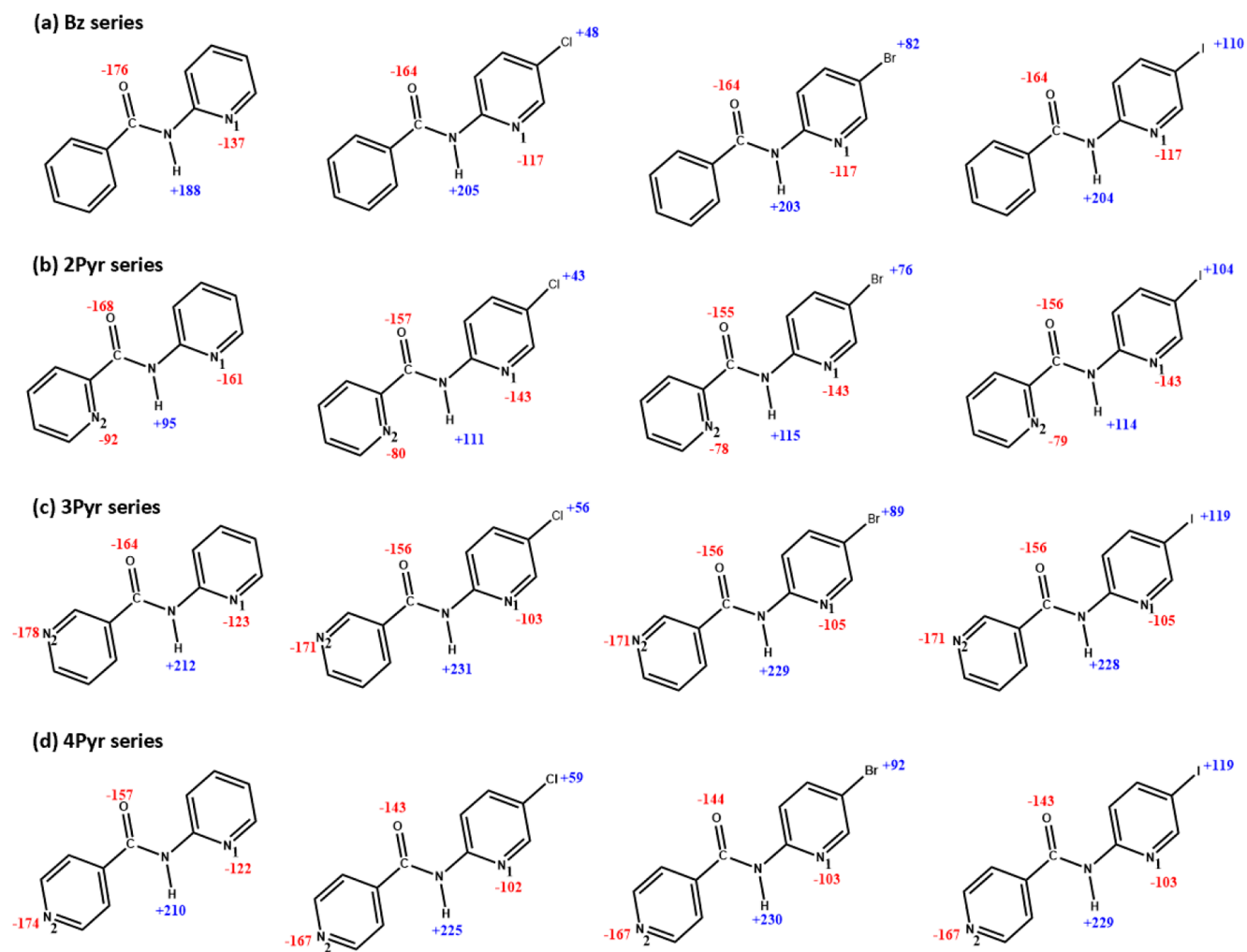


Figure 4. MEP values (kJ/mol) at the most likely donor and acceptor sites in the 16 target compounds.

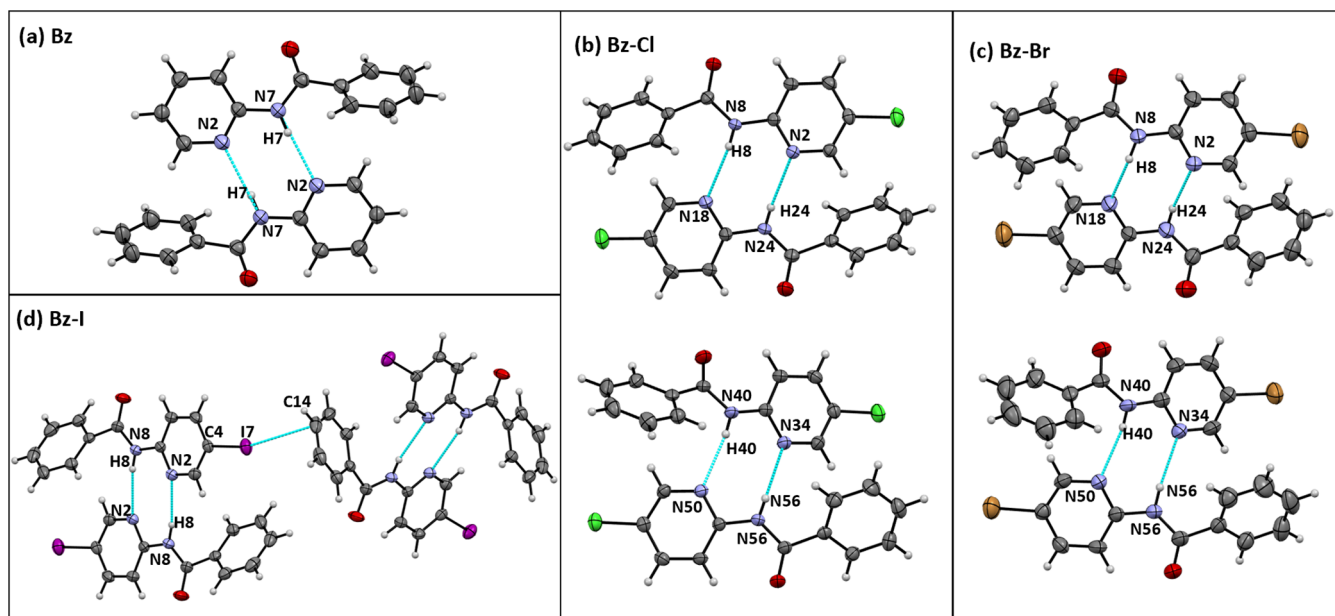


Figure 5. Primary interactions seen in single-crystal structures of (a) Bz, (b) Bz-Cl, (c) Bz-Br, and (d) Bz-I.

Table 2. Hydrogen- and Halogen-Bond Parameters of Crystal Structures in the Bz Series

	D–H/I...A	D/I...A (Å)	D–H...A (deg)
Bz	N7–H7...N2	3.0557(16)	166.5(16)
Bz-Cl	N8–H8...N18	3.189(2)	153.3(19)
	N24–H24...N2	3.203(2)	152(2)
	N40–H40...N50	2.967(2)	159.9(19)
	N56–H56...N34	3.108(2)	163.5(19)
Bz-Br	N8–H8...N18	3.211(5)	150(5)
	N24–H24...N2	3.227(5)	150(5)
	N40–H40...N50	2.987(5)	149(3)
	N56–H56...N34	3.113(5)	156(4)
Bz-I	N8–H8...N2	3.238(3)	163(3)
	C4–I7...C14	3.580(3)	162.37(9)

prevents the formation of pairwise dimers in the solid state. Again, the iodo analogue is the only member of this group that displays a structure-directing halogen bond, and interestingly, the iodine atom acts as a halogen-bond donor and acceptor simultaneously. The relevant hydrogen- and halogen-bond geometries in these four crystal structures are given in Table 3.

In all four crystal structures of the 3Pyr series the primary noncovalent interaction is a N–H...N(py) synthon (Figure 7). There are no additional structure-directing interactions shown by any of the halogenated compounds. The *trans* conformation with respect to the two ring nitrogen atoms is the preferred option in three of the four structures, while 3Pyr-Br is the only compound showing a *cis* arrangement. The relevant hydrogen- and halogen-bond geometries in these four crystal structures are given in Table 4.

The primary noncovalent interactions in the crystal structures from the 4Pyr series are shown in Figure 8. The primary hydrogen-bond interaction in 4Pyr is N–H...N(py) to the nitrogen N₂ (Figure 8). Both 4Pyr-Cl and 4Pyr-Br also follow this pattern in hydrogen bonding and form four-membered rings. In 4Pyr-I-i the halogen bond C–I...N to nitrogen N₂ and dimeric unit formation by the N–H...N(py)/N(py)...H–N

Table 3. Hydrogen- and Halogen-Bond Parameters of Crystal Structures in the 2Pyr Series

	D–H/I...A	D/I...A (Å)	D–H/I...A (deg)
2Pyr	N7–H7...N11	2.668(4)	113(4)
2Pyr-Cl	N8–H8...N12	2.647(3)	113(3)
2Pyr-Br	N8–H8...N12	2.645(4)	114(3)
2Pyr-I	N8–H8...N12	2.658(6)	115.(5)
	N24–H24...N28	2.655(6)	115.(5)
	C4–I7...N18	3.018(4)	176.06(17)
	C20–I23...I7	3.9173(5)	164.48(15)

synthon are seen. The C–I...N (to N₂) interaction is once again present in 4Pyr-I-ii, while the hydrogen-bond interaction changes to a N–H...O synthon. The relevant hydrogen- and halogen-bond geometries in these four crystal structures are given in Table 5.

The primary hydrogen and halogen bonds in the 16 crystal structures are summarized in Figure 9.

As can be seen from Figure 9, except for the two polymorphs of 4Pyr-I, the hydrogen bonds are identical among compounds within each series. To gain insight into the nature of the hydrogen bonding shown by these compounds in the solution phase, the chemical shift of the amide hydrogen in DMSO was investigated. The data appear clustered in three sets (Figure 10), and the connection between each of these sets to the crystal structures are addressed in detail in the Discussion.

DISCUSSION

We hypothesized initially that the Bz compounds would engage in one of two different synthons, N–H...O=C or N–H...N(py) hydrogen bonds, resulting in infinite chains or discrete dimers, respectively. In fact, in all four cases, only the latter interaction was observed in the solid state (Figure 9). A CSD search was conducted to compare the prevalence of this N–H...N(py)/N(py)...H–N interaction in molecules bearing a similar backbone: i.e., *N*-(pyridin-2-yl)benzamide. To make the analysis most relevant to our systems, only molecules with a single *N*-

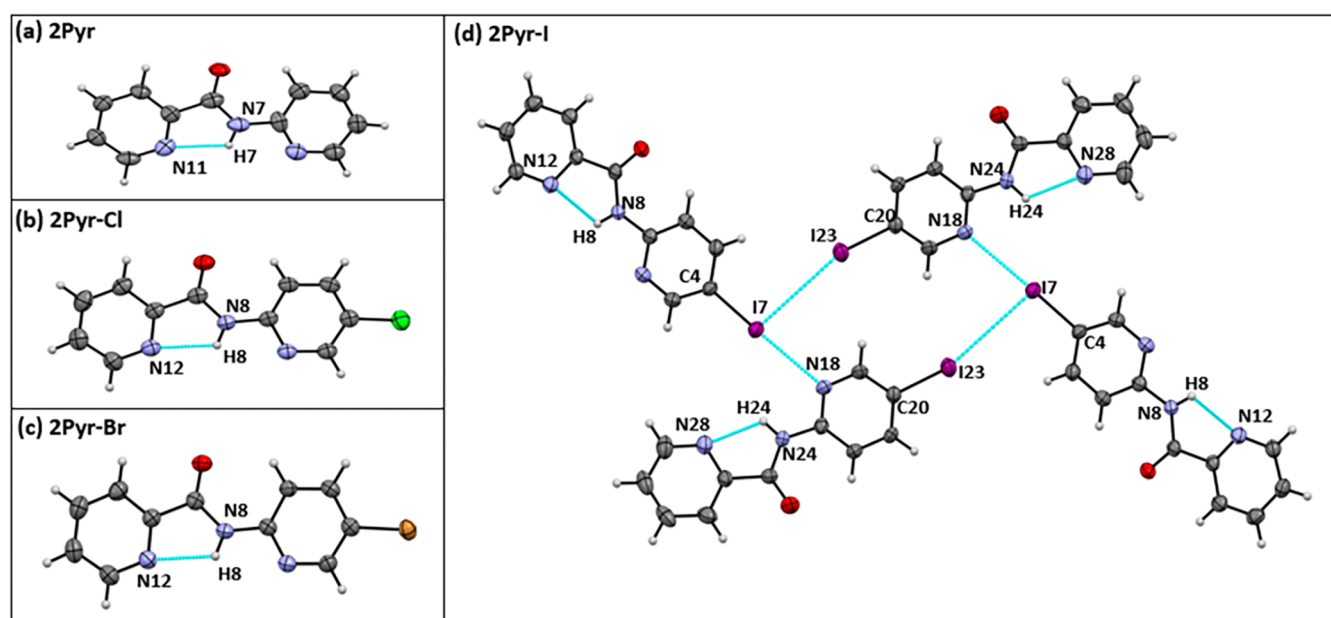


Figure 6. Primary interactions seen in single-crystal structures of (a) 2Pyr, (b) 2Pyr-Cl, (c) 2Pyr-Br, and (d) 2Pyr-I.

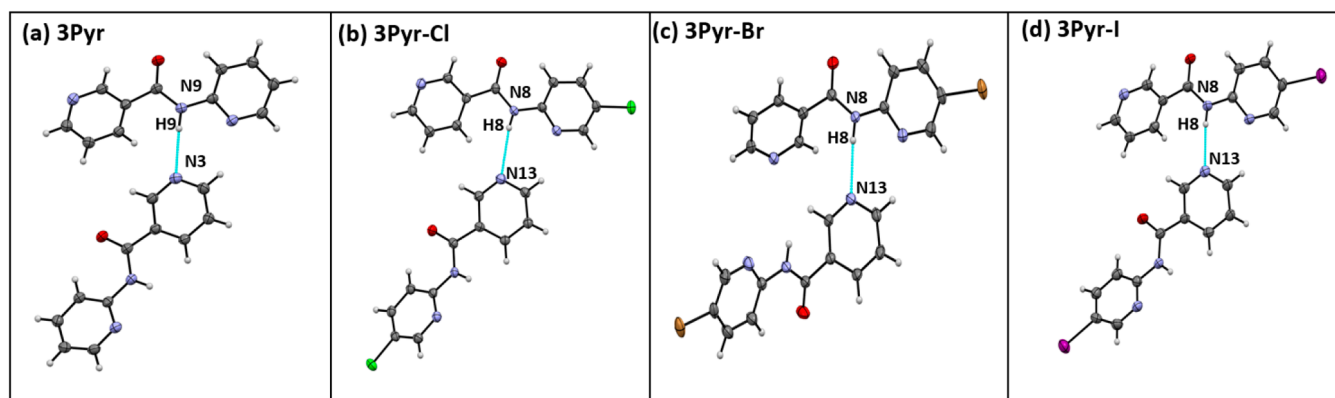


Figure 7. Primary interactions seen in single-crystal structures of (a) 3Pyr, (b) 3Pyr-Cl, (c) 3Pyr-Br, and (d) 3Pyr-I.

Table 4. Hydrogen- and Halogen-Bond Parameters of Crystal Structures in the 3Pyr Series

	D–H/I...A	D/I...A (Å)	D–H/I...A (deg)
3Pyr	N9–H9...N3	3.154(2)	176(2)
3Pyr-Cl	N8–H8...N13	3.233(2)	171(2)
3Pyr-Br	N8–H8...N13	3.079(3)	172(3)
3Pyr-I	N8–H8...N13	3.035(11)	169(9)

(pyridin-2-yl)benzamide unit and without any other potential hydrogen-bond donors (such as OH) or acceptors were included. The search identified 22 structures, and all but three of them contain the N–H...N(py)/N(py)...H–N interaction. In the three “outliers” (YOVKIG, JIXCUO, and JIXDAV) the N–H...O=C interaction is present instead. The refcodes for all 22 structures are given in Table S2 in the Supporting Information. Thus, the combined percentage for dimers in all 26 structures under consideration here is 88%, while the chain formation is 12%. The dominant assembly observed in the

Table 5. Hydrogen- and Halogen-Bond Parameters of Crystal Structures in the 4Pyr Series

	D–H/I...A	D/I...A (Å)	D–H/I...A (deg)
4Pyr	N17–H17...N11	3.3308(12)	170.1(11)
4Pyr-Cl	N8–H8...N14	3.0169(18)	179.0(19)
4Pyr-Br	N8–H8...N14	2.997(3)	171.(2)
4Pyr-I-i	N8–H8...N2	3.011(3)	166.(5)
	C4–I7...N14	3.013(2)	177.95(9)
4Pyr-I-ii	N9–H9... O8	3.086(13)	147.(12)
	C13–I16...N4	2.998(9)	171.5(4)
	N25–H25...O24	3.129(13)	171.(15)
	C29–I32...N20	2.969(10)	177.4(4)

solution phase is likely to serve as an important precursor to or indication of what will ultimately appear in the solid state and vice versa.³⁹ Separate NMR signals which may arise due to different synthons at play are averaged out in the resultant spectrum. All of the N–H peaks of compounds in this series

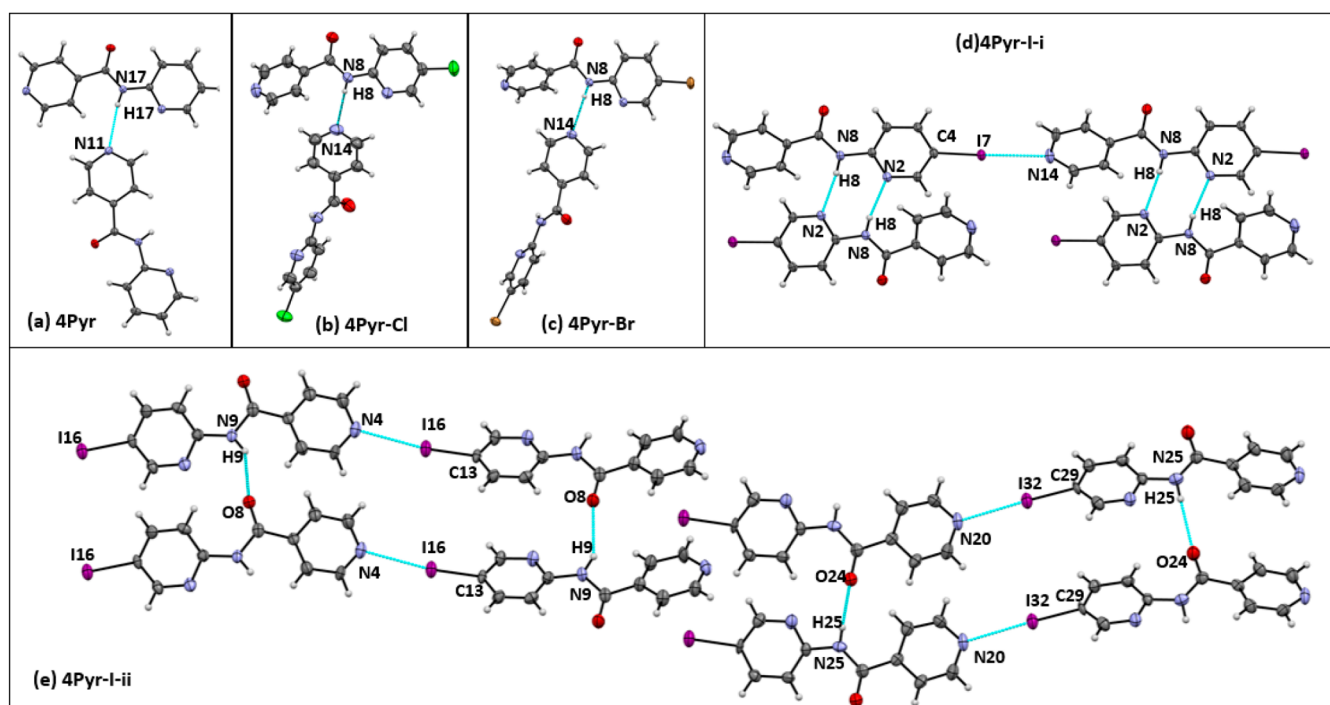


Figure 8. Primary interactions seen in single-crystal structures of (a) 4Pyr, (b) 4Pyr-Cl, (c) 4Pyr-Br, (d) 4Pyr-I-i, and (e) 4Pyr-I-ii.

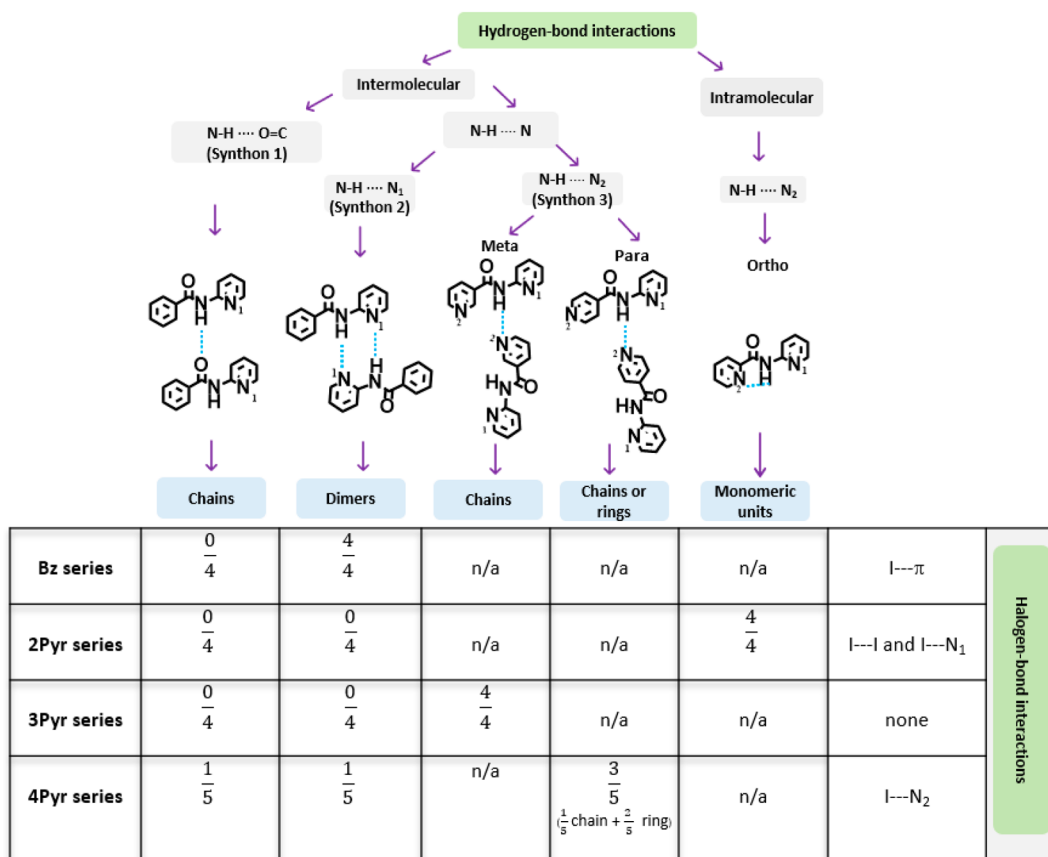


Figure 9. Summary of the primary hydrogen- and halogen-bond interactions in the 16 compounds.

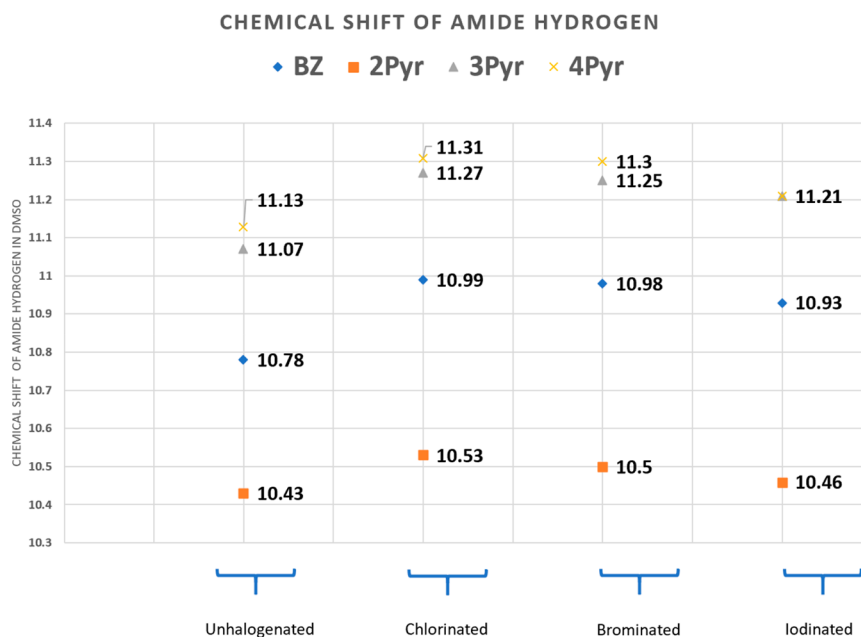


Figure 10. ¹H NMR chemical shift of the amide hydrogen atoms grouped by series.

occur within a 0.20 ppm range and are in a separate “band” in comparison to the other series (Figure 10). We can therefore confidently assume that the NMR data for all Bz compounds in this series indicate that they are similar to each other and predominantly form dimers in DMSO.

In the Bz series, the introduction of the halogen atoms altered the MEP of the donor and acceptor sites by increasing the donor potential and reducing the acceptor potential (less negative). The presence of electron-withdrawing groups is known to decrease electron density from donor sites, making them potentially stronger donors while the electron withdrawal from

acceptor sites lead to decreased electron density and weaker acceptors. Thus, in this case the electron-withdrawing nature of the halogen atom leads to the observed alterations of molecular electrostatic potentials.⁴⁰ Despite this, the N–H...N synthon was favored, resulting in dimer formation in each of the four cases. As the reported crystal structures also have varying MEP at the donor and acceptor sites it is clear that changes in the MEP potential at these sites do not lead to a change in the resulting supramolecular assembly. However, in the crystal structure of **Bz-I**, an additional interaction, an iodine– π halogen bond, is also present. The relatively limited polarizability of the chlorine and bromine analogues explains why similar short contacts did not appear in **Bz-Cl** and **Bz-Br**, respectively. **Bz-Cl** and **Bz-Br** are also isostructural.⁴¹ The I... π halogen bond is unlikely to be very strong, as it has not been “activated” through electron-withdrawing groups⁴² or via an sp-hybridized carbon atom.⁴³

In the **2Pyr** series, all four compounds showed intramolecular hydrogen bonding to N₂. The free rotation about the ring provides the perfect orientation between N₂ and the amide hydrogen for intramolecular hydrogen bonding. Even though the electrostatic potential on N₂ is higher than that of N₁, an intramolecular hydrogen bond is generally going to be favored over intermolecular hydrogen bonds. Again, the chloro and bromo compounds are isostructural with each other. The CSD analysis of the core **2Pyr** structure reveals the presence of the basic *N*-(pyridin-2-yl)picolinamide unit as a subunit in larger molecules, wherein the intramolecular hydrogen bonding has been used for constructing functional materials such as aqua pores (EPIDEO)⁴⁴ or pharmaceutical agents (FIDROB).⁴⁵ In **2Pyr-I** the vacant N₁ acts as a halogen-bond acceptor to an iodine atom on an adjacent molecule. The negatively charged “equator” of the same donor iodine acts as a halogen bond acceptor to another **2Pyr-I** molecule. Thus, there are two crystallographically unique **2Pyr-I** molecules in this structure. This also serves to explain the presence of two amide hydrogen peaks in the infrared spectrum (Figure S3). Once again, the increased polarizability of the iodine atom in comparison to the other halogen atoms enabled it to act as a halogen-bond donor while chlorine and bromine did not. The solution-phase NMR data indicated the absence of multiple assembly modes by the amide hydrogen. Moreover, the amide peaks of the compounds in this series occur in a different “band” in comparison to the other series. This indicates that the solution-phase assembly is quite distinct from those of the other series and reflects the nature of the observed outcome in the solid state. The NMR data also indicate that there are no dimers present in solution as was the case with the **Bz** compounds.

With shifting of the second pyridyl site in **3Pyr**, intramolecular hydrogen bonding is no longer an option. The postulated possibilities for hydrogen bonding were via synthon 1, synthon 2, or synthon 3. Synthon 3 is observed in all four structures in the solid state. Despite the donor potential of the amide hydrogen increasing and the acceptor potential decreasing with the introduction of the halogen, the same motif is observed throughout the series. The selection of synthon 3 over synthon 2 can be rationalized on the basis of the higher negative electrostatic potential of the acceptor nitrogen.²⁰ The CSD structure analysis revealed one compound, 2-chloro-*N*-(6-methyl-2-pyridinyl)nicotinamide (MEDJUB),⁴⁶ where the molecules assemble via synthon 3. In this compound the two pyridyl nitrogen atoms are arranged *cis* to each other. **3Pyr-Br** in this study was the only structure out of the four to also show a *cis* arrangement of the pyridyl nitrogen atoms. The

solution-phase NMR shows that all four compounds behave similarly. The chemical shift range for the compounds in this series are quite distinct from those observed for the **Bz** and **2Pyr** series. This nature of the difference in the synthon is also reflected in the solid state.

The expected synthons for the **4Pyr** series were synthon 1, synthon 2, or synthon 3. **4Pyr**, **4Pyr-Cl**, and **4Pyr-Br** assemble via synthon 3. In this series too, the chloro and bromo compounds exhibit isostructurality. All halogen atoms produced a similar alteration of the potentials at the amide hydrogen (making it stronger) and the acceptor sites (making them weaker). Despite this change, the hydrogen-bond synthon remained identical in these three compounds. We obtained two crystal structures for **4Pyr-I**, both of which showed different hydrogen bonding in comparison to the other compounds in the series. In **4Pyr-I-i** synthon 2 is observed and halogen bonding between iodine and N₂ is seen. The other polymorph, **4Pyr-I-ii**, was obtained from a failed cocrystallization experiment between **4Pyr-I** and dodecanoic acid. In **4Pyr-I-ii**, again halogen bond formation between iodine and N₂ is seen. The solution-phase data (NMR) indicate that the amide hydrogen appeared clustered in the same general range as in the **3Pyr** series. This similarity of the binding mode observed in the solution phase is also reflected in the solid state as all these compounds (except for **4Pyr-I**) assemble via synthon 3. The NMR of **4Pyr** is from a crystal of **4Pyr-I-i**. Although the amide hydrogen forms dimers in **4Pyr-I-i**, they are not “isolated” dimers as in the case of the **Bz** series. This may explain why it appears more downfield than for compounds in the **Bz** series. Additionally, the deviation of chemical shift to the bromo and chloro compounds in the series is different from the deviation of the other series (nearly 0.09 vs 0.05), and it may also reflect the chemical nature of the amide hydrogen due to the presence of synthon 1 seen in **4Pyr-I-ii**.

3Pyr-I was the only iodinated compound that did not show any halogen bonds or close contacts. In order to verify that the crystal of **3Pyr-I** grown is representative of the solid-state arrangement of the compound, experimental and simulated PXRDs were examined (Figure S4). The experimental PXRD did not reveal additional crystalline forms. The MEP value of the iodine in **3Pyr-I** is more positive than the iodinated compounds in the **Bz** and **2Pyr** series and is identical with that of **4Pyr-I**. Thus, the absence of any halogen bond or contact formation by **3Pyr-I** may be due to steric effects.

CONCLUSIONS

We find that the head-to-head dimer is the prevailing interaction in compounds of the **Bz** series in the four compounds of this study and among *N*-(pyridin-2-yl)benzamide compounds reported in the literature. With the introduction of the halogen in all series the acceptors became weaker and the donor stronger. On consideration of all four series, irrespective of which halogen atom within a series, the electrostatics at each donor and acceptor site is altered to the same extent: i.e., the MEP at the acceptor sites (carbonyl oxygen and pyridine nitrogen) is less negative and the donor potential (of the amide hydrogen) is increased in comparison to the nonhalogenated compound. In three out of the four series (**Bz**, **2Pyr**, and **4Pyr**) the chloro and bromo compounds are isostructural. Out of the 13 crystal structures obtained for the halogenated compounds, despite the MEP changes, the hydrogen-bonding motif was altered in only 2 out of 13 (2/13) structures with respect to the nonhalogenated compound. Although the hydrogen-bond motif was not altered, both **Bz-I** and **2Pyr-I** showed halogen-bond/contact formation.

Overall, only the iodinated targets exhibit halogen-bond/contact formation. This observation is in accordance with the halogen-bonding theory, where a higher polarizability of the halogen atom leads to a larger σ hole, as reflected in the calculated MEPs. Thus, the introduction of a halogen atom leads to significant changes in assembly in 4/13 cases, and all the changes occurred in the presence of the iodine substituent. It is worth noting that, in the case of **4Pyr-I**, halogen bonding occurs competitively with hydrogen bonding despite the iodine not being activated.

In these compounds, when another donor site of sufficient donor ability (iodine) is introduced, the overall assembly changes in comparison to the parent (unhalogenated) compounds. Since the hydrogen-bonding motif remained identical with those of the nonhalogenated, chlorinated, and brominated derivatives in 2/4 structures (**Bz-I** and **2Pyr-I**) and in the other 2/4 cases (both of the **4PyrI** structures) the hydrogen bond motif is different, the halogen-bonding iodine site acted as an auxiliary donor 50% of the time and as a competitor 50% of the time to the amide hydrogen (Figure 11).

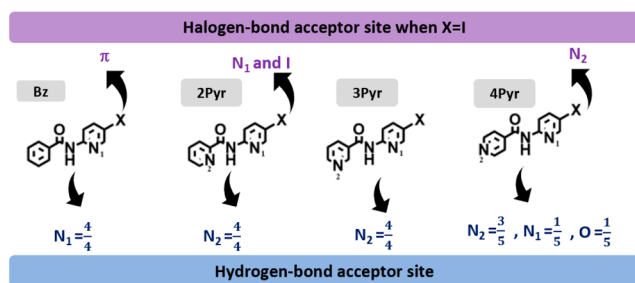


Figure 11. Summary of the motifs in the 16 compounds analyzed herein, grouped by series.

■ ASSOCIATED CONTENT

Supporting Information

The Supporting Information is available free of charge at <https://pubs.acs.org/doi/10.1021/acs.cgd.0c01086>.

Crystallographic data, refcodes of *N*-(pyridin-2-yl)-benzamide structures from the CCDC, FT-IR spectrum of **2Pyr-I**, and PXRD data of **3Pyr-I** (PDF)

Accession Codes

CCDC 2021116–2021132 contain the supplementary crystallographic data for this paper. These data can be obtained free of charge via www.ccdc.cam.ac.uk/data_request/cif, or by emailing data_request@ccdc.cam.ac.uk, or by contacting The Cambridge Crystallographic Data Centre, 12 Union Road, Cambridge CB2 1EZ, UK; fax: +44 1223 336033.

■ AUTHOR INFORMATION

Corresponding Author

Christer B. Aakeröy – Department of Chemistry, Kansas State University, Manhattan, Kansas 66506, United States;
 orcid.org/0000-0002-8947-2068; Phone: +1-785-532-6096; Email: aakeroy@ksu.edu

Authors

Amila M. Abeysekera – Department of Chemistry, Kansas State University, Manhattan, Kansas 66506, United States
 Victor W. Day – University of Kansas, Chemistry Department, Lawrence, Kansas 66045, United States

Abhijeet S. Sinha – Department of Chemistry, Kansas State University, Manhattan, Kansas 66506, United States;
 orcid.org/0000-0001-5610-2848

Complete contact information is available at:
<https://pubs.acs.org/10.1021/acs.cgd.0c01086>

Notes

The authors declare no competing financial interest.

■ ACKNOWLEDGMENTS

A.M.A. acknowledges support from the Johnson Cancer Research Center at Kansas State University and General Sir John Kotelawala Defence University. V.W.D. acknowledges the NSF-MRI grant CHE-0923449, which was used to purchase an X-ray diffractometer and software used in this study. We thank Dr. S. P. Panikkattu for the crystal growth of **4Pyr**.

■ REFERENCES

- (1) Steiner, T. The hydrogen bond in the solid state. *Angew. Chem., Int. Ed.* **2002**, *41*, 48–76.
- (2) Hisaki, I.; Suzuki, Y.; Gomez, E.; Ji, Q.; Tohna, N.; Nakamura, T.; Douhal, A. Acid responsive hydrogen-bonded organic frameworks. *J. Am. Chem. Soc.* **2019**, *141*, 2111–2121.
- (3) Wang, H.; Bisoyi, H. K.; Urbas, A. M.; Bunning, T. J.; Li, Q. The halogen bond: an emerging supramolecular tool in the design of functional mesomorphic materials. *Chem. - Eur. J.* **2019**, *25*, 1369–1378.
- (4) Meazza, L.; Foster, J. A.; Fucke, K.; Metrangolo, P.; Resnati, G.; Steed, J. W. Halogen-bonding-triggered supramolecular gel formation. *Nat. Chem.* **2013**, *5*, 42–47.
- (5) Scilabra, P.; Terraneo, G.; Resnati, G. The chalcogen bond in crystalline solids: A world parallel to halogen bond. *Acc. Chem. Res.* **2019**, *52*, 1313–1324.
- (6) Vogel, L.; Wonner, P.; Huber, S. M. Chalcogen bonding: An overview. *Angew. Chem., Int. Ed.* **2019**, *58*, 1880–1891.
- (7) Resnati, G.; Boldyreva, E.; Bombicz, P.; Kawano, P. Supramolecular interactions in the solid-state. *IUCrJ* **2015**, *2*, 675–690.
- (8) Aakeröy, C. B.; Wijethunga, T. K.; Desper, J. Constructing molecular polyions using halogen bonding and bifurcated N-oxides. *CrystEngComm* **2014**, *16*, 28–31.
- (9) Mandal, S.; Mukhopadhyay, T. K.; Mandal, N.; Datta, A. Hierarchical Noncovalent Interactions between Molecules Stabilize Multicomponent Cocrystals. *Cryst. Growth Des.* **2019**, *19*, 4802–4809.
- (10) Babu, N. J.; Cherukuvada, S.; Thakuria, R.; Nangia, A. Conformational and synthon polymorphism in furosemide (Lasix). *Cryst. Growth Des.* **2010**, *10*, 1979–1989.
- (11) Gong, N.; Yang, D.; Jin, G.; Liu, S.; Du, G.; Lu, Y. Structure, characterization, solubility and stability of podophyllotoxin polymorphs. *J. Mol. Struct.* **2019**, *1195*, 323–330.
- (12) Kavanagh, O. N.; Croker, D. M.; Walker, G. M.; Zaworotko, M. J. Pharmaceutical cocrystals: from serendipity to design to application. *Drug Discovery Today* **2019**, *24*, 796–804.
- (13) Kacso, I.; Rus, L. M.; Martin, F.; Miclaus, M.; Filip, X.; Dan, M. Solid-state compatibility studies of Ketoconazole-Fumaric acid cocrystal with tablet excipients. *J. Therm. Anal. Calorim.* **2020**, 1–8.
- (14) Goldyn, M.; Larowska, D.; Nowak, W.; Bartoszak-Adamska, E. Synthon hierarchy in theobromine cocrystals with hydroxybenzoic acids as cofomers. *CrystEngComm* **2019**, *21*, 7373–738.
- (15) Desiraju, G. R. Supramolecular synthons in crystal engineering—a new organic synthesis. *Angew. Chem., Int. Ed. Engl.* **1995**, *34*, 2311–2327.
- (16) Corpinot, M. K.; Bučar, D. K. A Practical guide to the design of molecular crystals. *Cryst. Growth Des.* **2019**, *19*, 1426–1453.
- (17) Khavasi, H. R.; Hosseini, M.; Tehrani, A. A.; Naderi, S. Strengthening N...X halogen bonding via nitrogen substitution in the aromatic framework of halogen-substituted arylpyrazinamides. *CrystEngComm* **2014**, *16*, 4546–4553.

- (18) Liu, H.; Yang, X.; Chen, J.; Zhang, M.; Parkin, S.; Cao, S.; Li, T.; Yang, Z.; Yu, F.; Long, S. Steric Effect Determines the Formation of Lactam-Lactam Dimer or Amide C=O...NH (Lactam) Chain Motif in N-phenyl-2-hydroxynicotinanilides. *Cryst. Growth Des.* **2020**, *20*, 4346–4357.
- (19) Goswami, A.; Garai, M.; Biradha, K. Interplay of halogen bonding and hydrogen bonding in the cocrystals and salts of dihalogens and trihalides with N, N'-bis (3-pyridylacrylamido) derivatives: phosphorescent organic salts. *Cryst. Growth Des.* **2019**, *19*, 2175–2188.
- (20) Perera, M. D.; Desper, J.; Sinha, A. S.; Aakeröy, C. B. Impact and importance of electrostatic potential calculations for predicting structural patterns of hydrogen and halogen bonding. *CrystEngComm* **2016**, *18*, 8631–8636.
- (21) Mocilac, P.; Tallon, M.; Lough, A. J.; Gallagher, J. F. Synthesis, structural and conformational analysis of a 3×3 isomer grid based on nine methyl-N-(pyridyl) benzamides. *CrystEngComm* **2010**, *12*, 3080–309.
- (22) Mocilac, P.; Donnelly, K.; Gallagher, J. F. Structural systematics and conformational analyses of a 3×3 isomer grid of fluoro-n-(pyridyl) benzamides: Physicochemical correlations, polymorphism and isomorphous relationships. *Acta Crystallogr., Sect. B: Struct. Sci.* **2012**, *68*, 189–203.
- (23) Gallagher, J. F.; Farrell, M.; Hehir, N.; Mocilac, P.; Aubert, E.; Espinosa, E.; Benoit, G.; Jelsch, C. At the Interface of Isomorphous Behavior in a 3×3 Isomer Grid of Monochlorobenzamides: Analyses of the Interaction Landscapes via Contact Enrichment Studies. *Cryst. Growth Des.* **2019**, *19*, 6141–6158.
- (24) Wolters, L. P.; Schyman, P.; Pavan, M. J.; Jorgensen, W. L.; Bickelhaupt, F. M.; Kozuch, S. The many faces of halogen bonding: a review of theoretical models and methods. *Wiley Interdisciplinary Reviews: Computational Molecular Science* **2014**, *4*, 523–540.
- (25) The Cambridge Structural Database: Groom, C. R.; Bruno, I. J.; Lightfoot, M. P.; Ward, S. C. *Acta Crystallogr., Sect. B: Struct. Sci., Cryst. Eng. Mater.* **2016**, *B72*, 171–179.
- (26) Liu, Y. Z.; Wang, H.; Chan, C. K.; Mu, X.; Robeyns, K.; Wang, C. C.; Singleton, M. L. Structure-Dependent Guest Recognition with Flexible Ferrocene-Based Aromatic Oligoamide β -Sheet Mimics. *Chem. - Eur. J.* **2020**, *26*, 181–185.
- (27) Gan, Q.; Ferrand, Y.; Bao, C.; Kauffmann, B.; Grélard, A.; Jiang, H.; Huc, I. Helix-rod host-guest complexes with shuttling rates much faster than disassembly. *Science* **2011**, *331*, 1172–1175.
- (28) McMoran, E. P.; Dominguez, M. N.; Erwin, E. M.; Powell, D. R.; Rowe, G. T.; Yang, L. Structural diversity, spectral characterization and computational studies of Cu (I) complexes with pyridylamide ligands. *Inorg. Chim. Acta* **2016**, *446*, 150–160.
- (29) Rai, D.; Singh, R. K. Synthesis and antibacterial activity of benzamides and sulfonamide derived from 2-amino-5-bromo/nitro-pyridine against bacterial strains isolated from clinical patients. *Indian J. Chem.* **2011**, *50B*, 931–936.
- (30) Yang, S.; Yan, H.; Ren, X.; Shi, X.; Li, J.; Wang, Y.; Huang, G. Copper-catalyzed dehydrogenative reaction: synthesis of amide from aldehydes and aminopyridine. *Tetrahedron* **2013**, *69*, 6431–6435.
- (31) Nicolas, L.; Angibaud, P.; Stansfield, I.; Meerpoel, L.; Reymond, S.; Cossy, J. Copper-catalysed amidation of 2-chloro-pyridines. *RSC Adv.* **2013**, *3*, 18787–18790.
- (32) This reported melting point of this compound is likely to be in error.
- (33) Searls, T.; Chen, D. L.; Lan, T.; McLaughlin, L. W. Nucleoside Analogue Substitutions in the Trinucleotide DNA Template Recognition Sequence 3'-(CTG)-5' and Their Effects on the Activity of Bacteriophage T7 Primase. *Biochemistry* **2000**, *39*, 4375–4382.
- (34) Vu, H. N.; Kim, J. Y.; Hassan, A. H.; Choi, K.; Park, J. H.; Park, K. D.; Lee, J. K.; Pae, A. N.; Choo, H.; Min, S. J.; Cho, Y. S. Synthesis and biological evaluation of picolinamides and thiazole-2-carboxamides as mGluR5 (metabotropic glutamate receptor 5) antagonists. *Bioorg. Med. Chem. Lett.* **2016**, *26*, 140–144.
- (35) Wang, K.; Shen, M.; Sun, W. H. N-(Pyridin-2-yl) picolinamide tetranickel clusters: Synthesis, structure and ethylene oligomerization. *Polyhedron* **2010**, *29*, 564–568.
- (36) Aakeröy, C. B.; Panikkattu, S. V.; DeHaven, B.; Desper, J. Establishing supramolecular control over solid-state architectures: a simple mix and match strategy. *Cryst. Growth Des.* **2012**, *12*, 2579–2587.
- (37) The crystal structure of this compound was reported during the course of this project: Pappula, V.; Ravi, C.; Samanta, S.; Adimurthy, S. Oxidative Amidation of Methylarenes and Heteroamines under Metal-Free Conditions. *Chem. Select Comm.* **2017**, *2*, 5887–5890.
- (38) Kumar, D. K.; Jose, D. A.; Dastidar, P.; Das, A. Nonpolymeric hydrogelator derived from N-(4-pyridyl) isonicotinamide. *Langmuir* **2004**, *20*, 10413–10418.
- (39) Osmialowski, B.; Kolehmainen, E.; Dobosz, R.; Gawinecki, R.; Kauppinen, R.; Valkonen, A.; Juha, K.; Rissanen, K. (2010). Self-organization of 2-acylaminopyridines in the solid state and in solution. *J. Phys. Chem. A* **2010**, *114*, 10421–10426.
- (40) Aakeröy, C. B.; Rajbanshi, A.; Li, Z. J.; Desper, J. Mapping out the synthetic landscape for re-crystallization, co-crystallization and salt formation. *CrystEngComm* **2010**, *12*, 4231–4239.
- (41) Mukherjee, A.; Desiraju, G. R. Halogen bonds in some dihalogenated phenols: applications to crystal engineering. *IUCrJ* **2014**, *1*, 49–60.
- (42) Bamberger, J.; Ostler, F.; Mancheño, O. G. Frontiers in Halogen and Chalcogen-Bond Donor Organocatalysis. *ChemCatChem* **2019**, *11*, 5198–5211.
- (43) Bosch, E.; Kruse, S. J.; Groeneman, R. H. Infinite and discrete halogen bonded assemblies based upon 1, 2-bis (iodoethynyl) benzene. *CrystEngComm* **2019**, *21*, 990–993.
- (44) Zhao, H.; Sheng, S.; Hong, Y.; Zeng, H. Proton gradient-induced water transport mediated by water wires inside narrow aquapores of aquafoldamer molecules. *J. Am. Chem. Soc.* **2014**, *136*, 14270–14276.
- (45) Gottschalk, S.; Engelmann, J.; Rolla, G. A.; Botta, M.; Parker, D.; Mishra, A. Comparative in vitro studies of MR imaging probes for metabotropic glutamate subtype-5 receptor targeting. *Org. Biomol. Chem.* **2013**, *11*, 6131–6141.
- (46) Fernandes, E. L.; Magalhaes, A.; Paes, K. C.; De Souza, M. V.; Vasconcelos, T. R.; Wardell, J. L.; Wardell, S. M. Cyclisation of 2-Chloro-N-(2-Pyridinyl) Nicotinamides to 5-Oxo-5, 6-Dihydrodipyrido [1, 2-a: 3', 2'-e] Pyrimidin-11-Ium Chlorides. *J. Chem. Res.* **2006**, *2006*, 93–97.